S.K. SAHU[1], N.K. KUND[1*]

IMPACT OF COOLANT WATER FLOW RATE AND TEMPERATURE UNDERSIDE COOLING SLOPE ON SOLIDIFICATION WITH MICROSTRUCTURE AND MECHANICAL PROPERTIES OF CASTED AZ91 MG ALLOY

Present study describes about the effect of coolant water flow rate and coolant water temperature underside cooling slope on structural characteristics of casted AZ91 Mg alloy. Here, over the cooling slope, hot melt flows from top to bottom. Additionally, under the cooling slope, coolant water flows from bottom to top. Slurry gets obtained at bottom of cooling slope by pouring AZ91 Mg melt from top of the slope. Coolant water flow rate with coolant water temperature underside cooling slope warrant necessary solidification and shear to obtain AZ91 Mg slurry. Specifically, slurry at 5 different coolant water flow rates (4, 6, 8, 10, 12 lpm) and at 5 different coolant water temperatures (15, 20, 25, 30, 35°C) underside cooling slope are delivered inside metal mould. Modest coolant water flow rate of 8 lpm with coolant water temperature of 25°C (underside cooling slope) results fairly modest solidification that would enormously contribute towards enhanced structural characteristics. As, quite smaller/bigger coolant water flow rate/temperature underside cooling slope would reason shearing that causes inferior structural characteristics. Ultimately, favoured microstructure was realized at 8 lpm coolant water flow rate and 25°C coolant water temperature underside cooling slope with grain size, shape factor, primary α-phase fraction and grain density of 63 µm, 0.71, 0.68 and 198, respectively. Correspondingly, superior mechanical properties was realized at 8 lpm coolant water flow rate and 25°C coolant water temperature underside cooling slope with tensile strength, elongation, yield strength and hardness of 250 MPa, 8%, 192 MPa and 80 HV, respectively.

Keywords: Coolant water flow rate; Coolant water temperature; Cooling slope; Microstructure; Mechanical properties

1. Introduction

On account of tough environmental guidelines across the sphere, the thriving focus always stays at bringing out eco-friendly materials with superior strength, decreased weight, higher potential and greater safety. Due to the mentioned demands, light weighting is mandatory but not optional. In addition, outgoing works on cell run vehicles, natural fuels and biotechnology too supplement secondary burden of weight. For example, hybrid electric vehicle uses less fuel than conventional one. Since, that uses electric-drive technology for enhancing its performance by regenerative braking. Furthermore, practice with typical high speed steel (HSS), tailor welded blank (TWB) or hot press would never serve the purpose. Hence, materials lighter than HSS having enhanced strength definitely remain vital [1-3]. As a result, magnesium alloys stay widely utilized as impending type materials for numerous household and engineering practices. Yet, it remains 33% lighter than aluminium alloys [3]. Correspondingly, magnesium alloys are subjected to various thermal and mechanical practices. However, casting stands as a basic method for Mg alloys production.

In addition, studies on microstructures of squeeze casting of light alloys/composites are also reported in texts [4]. Parametric effects of mold or die casting on strength or creep of behaviors of AZ91D was also described [5]. Besides, parametric effects on thermal behaviours of high pressure die casting (HPDC) of Mg alloys have also been investigated [6]. Rheological properties pertaining to viscosity and shear rate of AZ91 alloys at semisolid condition was investigated [7]. Comparative tribological properties relating to corrosion and wear behaviours of die-casted and injection moulded AZ91D alloy was examined [8]. Studies on microstructure of cooling slope (CS) cast and thixoformed Al alloy blocks was reported [9]. Additionally, details about semisolid materials (SSM) processing on structural behaviours was also described widely [10]. Structural properties of thixomolded and SSM processed Mg alloys were compared as well [11]. Studies on microstructures of CS casting of cast iron (CI) was also reported in literature [12]. Rheo-diecasting practice was also developed for billet casting of Mg alloys [13]. Besides, influence of melting practice on the structural characteristics of AZ91 Mg alloys was studied [14]. Investigations of microstructures on

---

[1] VSS UNIVERSITY OF TECHNOLOGY, DEPARTMENT OF PRODUCTION ENGINEERING, BURLA 768018, INDIA

* Corresponding author: nirmalkund@gmail.com

thixoformed and CS cast A357 alloy was also carried out [15]. Furthermore, studies on microstructures of CS cast A356 alloy is also reported in texts [16].

Microstructural properties of SSM casting of A356 alloy billets obtained via serpentine channel was also studied [17]. Influences of nozzle size/height and plate tilt/length on semisolid condition of CS cast A356 alloy was investigated as well [18]. Studies on quality of A356 alloy slurry produced through serpentine channel is also available [19]. Besides, studies on parametric influences (concerning casting temperature, roll speed, plate angle with vibration) on structural characteristics of CS strip cast AZ91/AZ31 alloy was also described [20,21]. Numerical studies on effects of pouring temperature, plate gradient/length alongside cooling rate on solidification behaviours of CS cast A356 alloy was also done [22,23]. Additionally, microstructure with mechanical characteristics of squeeze cast A356 alloy produced via vibrating CS was also examined [24]. Studies on microstructures of cast iron produced via cooling slope are also reported [25]. Studies on structural characteristics of CS cast ZCuSn10P1 alloy were also described [26]. Investigations were done on influences of process parameters on structural properties of CS cast A356 alloy produced by semisolid forming (SSF) [27]. Investigations on effects of plate length/tilt on production of CS cast A356/A380 alloy feedstocks were also done [28]. Studies on

optimization of pouring temperature for CS cast hypereutectic Al-Si alloy were described as well [29].

Very general cooling slope casting associated experimental investigations mentioned so far definitely involve some important process parameters as reported before in some texts. But, reported investigations completely suffer from non-appearance of *coolant water flow rate and coolant water temperature* underside cooling slope. To finest of authors' observations, there remain not a single experimental investigation on impact of coolant water flow rate and coolant water temperature underside cooling slope on solidification with microstructure and mechanical properties of casted AZ91 Mg alloy destined for CS semisolid casting. With this posture, present research establishes experimental studies on impact of coolant water flow rate and coolant water temperature underside cooling slope on solidification with microstructure and mechanical properties of casted AZ91 Mg alloy destined for CS semisolid casting.

2. Experimental

Fig. 1 depicts the experimental section (destined for carrying out investigations) that entails tundish, stainless steel cooling slope, water channel and stainless steel metal mould (to produce castings).
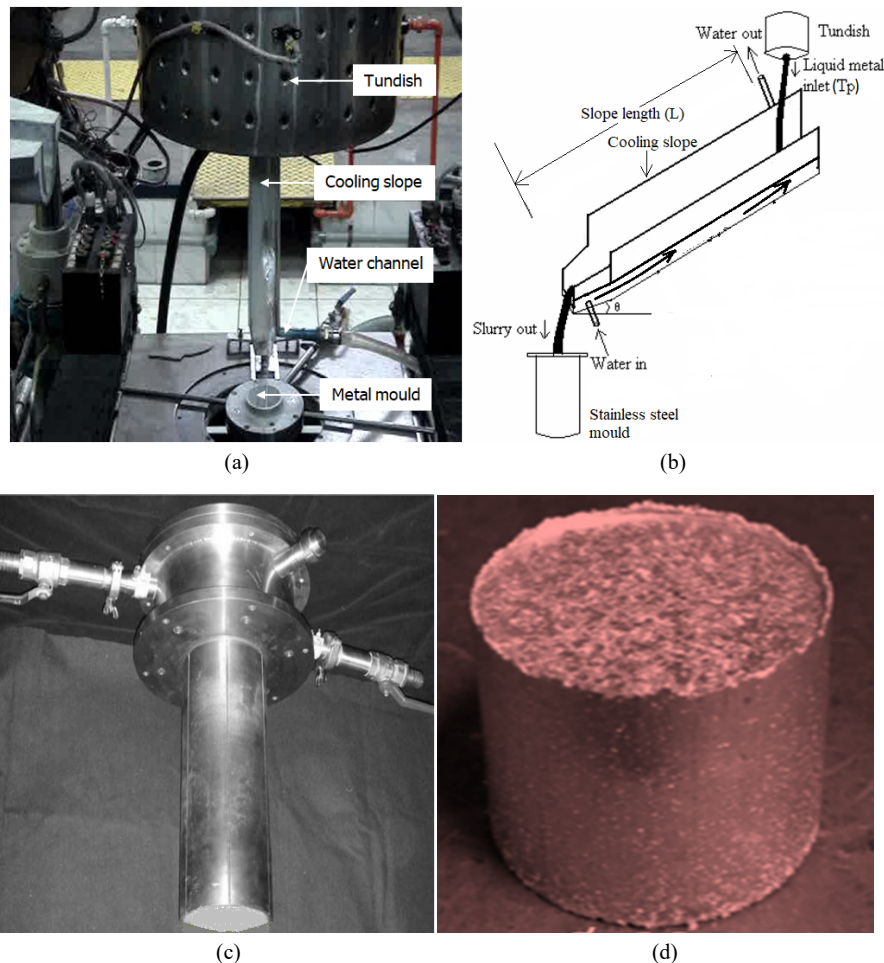

Fig. 1. Experimental section involving (a) photograph of setup, (b) schematic of setup, (c) photograph of metal mould and (d) photograph of a semisolid casting

2.1. Materials

Commonly used AZ91 alloy was deployed as test material in current study. Chemical composition of AZ91 alloy remains as (by wt.): 8.3-9.7%Al, 0.35-1%Zn, 0.2%Mn, 0.1%Si, 0.03%Cu, 0.002%Ni, 0.005%Fe and balance Mg. The liquidus and solidus temperatures of AZ91 alloy are just about 598°C and 470°C, respectively.

2.2. Melt preparation and treatment

AZ91 alloy pieces are utilized in present study. AZ91 alloy melt gets prepared within silicon-carbide crucible positioned inside resistance furnace. Besides, for appropriate grain modification/refinement, the melt undergoes chemicals treatments with carbides (for carbon inoculation) and other additive TiB_2. Information pertaining to melting with treating practices also illustrated previously [22,23].

2.3. Melt pouring and slurry production

Basically 1.5 kg of AZ91 alloy melt (at 605°C) was slowly released into metal mould using cooling slope of length 250 mm with gradient 60º. Specifically, alloy slurry at five diverse coolant water flow rates (4, 6, 8, 10 and 12 lpm) and at five diverse coolant water temperatures (15, 20, 25, 30 and 35 °C) underside cooling slope are delivered inside metal mould. With K-type thermocouple, temperature of alloy slurry at slope outlet too was recorded regularly. Information on melt pouring and slurry production too illustrated previously [22,23].

2.4. Sample preparation

Thick sample of 20 mm got shaped from all mould castings of AZ91 alloy. Various classes of emery papers got considered to enhance samples' surface features [22,23]. It succeeded with SiC powder and diamond paste polishing. In other words, each AZ91 alloy casting undergoes usual practices like cutting (using power hacksaw), grinding (using abrasive grinding wheel), normal polishing (using different grades of sandpapers) followed by SiC powder polishing alongside diamond paste polishing and etching (using appropriate acetic glycol solution), More appropriately, processed samples undergo etchant treatment using acetic glycol solution (20 ml acetic acid, 1 ml HNO_3, 60 ml ethylene glycol and 20 ml water). Lastly, samples undergo metallographic testing for optical microscopy.

2.5. Microstructural evaluation

Microstructural characterization on grain size, shape factor, primary α-phase fraction and grain density got carried out on samples' micrographs. In addition, particle shape factor (or globularity) is referred as $4\pi A/P^2$ i.e. $4\pi(\text{area})/(\text{perimeter})^2$. That ranges from 0 (for dendrite) to 1 (for circle). Furthermore, grain density (count/sq. mm) remains determined deploying Sigma Scan Pro (version 4.0) image analysis software. More information on micrograph and microstructural evaluation practices also illustrated previously [22,23].

2.6. Mechanical properties

Tensile samples of size 25×5 mm were shaped from all castings. Essential sample tests were accomplished by INSTRON 5567 showing 10^{-3}/s strain rate. Presently, EN ISO 6892-1 testing standard is used. In addition, hardness samples of dimension 40×20 mm were shaped from semisolid castings. Hardness tests were done using Zeiss UHL VMHT 0.001 Vickers hardness tester. Diamond indenter operates on load 1.96 N and dwell time 20 s. These tests were done to evaluate strength, elongation and hardness of AZ91 alloy castings.

3. Results and discussion

Comprehensive tests were carried out for experimental study on impact of coolant water flow rate and coolant water temperature underside cooling slope on solidification with microstructure and mechanical properties of casted AZ91 Mg alloy destined for CS semisolid casting. Present study conveys on perceptive moderate coolant water flow rate and temperature that would bring pretty modest solidification with microstructure and mechanical properties of cooling slope casting. Initially, for test case AZ91 alloy melt at 605°C temperature was discharged on cooling slope of 250 mm length and 60° gradient concerning 8 lpm coolant water flow rate along with 25°C coolant water temperature underside cooling slope.

3.1. Impact of coolant water flow rate underside cooling slope

For experimental investigation on impact of coolant water flow rate underside cooling slope on solidification with microstructure and mechanical properties, conscientious tests were carried out with generation of AZ91 alloy slurry (at slope outlet) for five diverse coolant water flow rates (4, 6, 8, 10 and 12 lpm) underside cooling slope. Elevated coolant water flow rate concerns less slurry temperature at slope outlet. Magnitude of solidification upsurges with coolant water flow rate owing to taking away of more heat by coolant water during the process. Therefore, solid fraction increases with coolant water flow rate underside cooling slope. Table 1 sums up temperature with solid fraction summary of alloy slurry released from slope outlet at five diverse coolant water flow rates underside cooling slope.

Temperature with solid fraction summary of AZ91 alloy slurry released from slope outlet at five diverse coolant water flow rates underside cooling slope

Coolant water flow rate underside cooling slope (lpm)	T_{outlet} (°C)	Solid fraction by Scheil equation (%)
4	592	15
6	589	20
8	582	24
10	578	29
12	576	32

3.1.1. Microstructure of semisolid castings

5 different castings were obtained at five different coolant water flow rates underside cooling slope. Samples were prepared to capture micrographs for metallographic study. Fig. 2 illustrates representative microstructures of mould castings of AZ91 alloy. It only discloses about variations in pragmatic morphology of castings obtained at different coolant water flow rates underside cooling slope. Besides, microstructural characterizations get performed deploying Sigma Scan Pro (version 4.0) image analysis software [22,23].

3.1.2. Structural characterization of semisolid castings

Fig. 3 shows structural characterization of previously depicted mould castings microstructures of AZ91 alloy. Pragmatic

that initially grain size reduces with increase in coolant water flow rate (underside cooling slope) till 8 lpm and then trend reverses. Whilst, shape factor, primary α-phase fraction, and grain density enhance with coolant water flow rate till 8 lpm and then trend reverses. As, firstly, shearing increases with coolant water flow rate underside cooling slope on account of nucleation and grain growth besides flow inertia. But, afterward, shearing decreases with further increase in coolant water flow rate underside cooling slope on account of particle sticking and deposition/accumulation besides flow inertia. Ultimately, favored microstructure got realized at 8 lpm coolant water flow rate underside cooling slope with grain size, shape factor, primary α-phase fraction and grain density of 63 μm, 0.71, 0.68 and 198, respectively.

3.1.3. Mechanical properties of semisolid castings

Fig. 4 shows mechanical properties of semisolid castings of AZ91 alloy. Pragmatic that initially strength, elongation and hardness increase with coolant water flow rate (underside cooling slope) till 8 lpm and later trend reverses. Mainly it occurs because of influence of grain refinement on mechanical properties that gets fully realized from Hall-Petch effect. Certainly, smaller grain causes higher strength, whilst, higher shape factor and/or homogeneity causes higher ductility. Ultimately, superior mechanical properties got realized at 8 lpm coolant water flow rate underside cooling slope with tensile strength, elongation, yield strength and hardness of 250 MPa, 8%, 192 MPa and 80 HV, respectively.
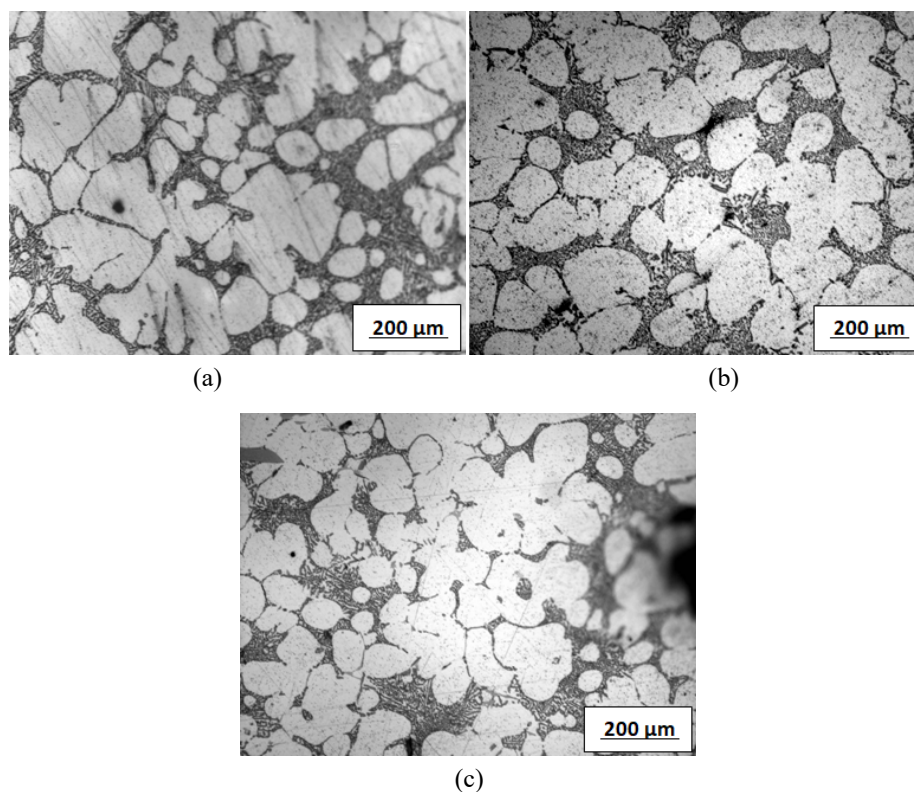

(a)

(b)

(c)

Fig. 2. Microstructures of semisolid castings obtained at coolant water flow rates (underside cooling slope) of (a) 4 lpm, (b) 8 lpm and (c) 12 lpm
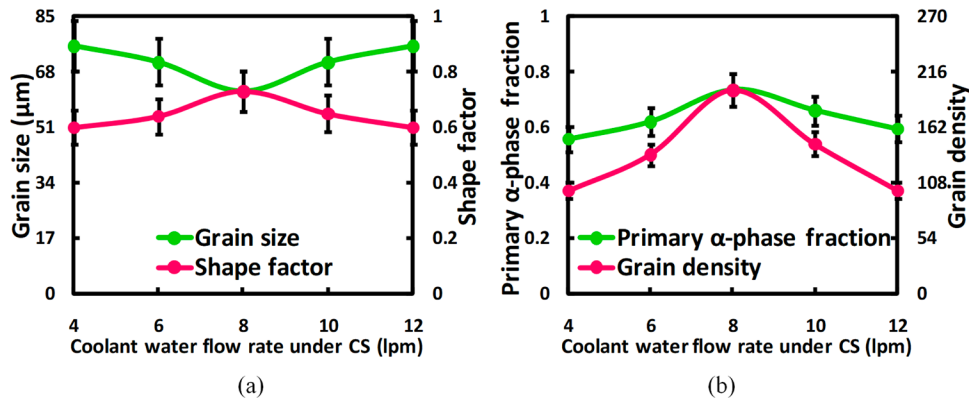
Fig. 3. Structural characterization of semisolid castings relating coolant water flow rates (underside cooling slope) with (a) grain size/shape factor and (b) α-phase fraction/grain density
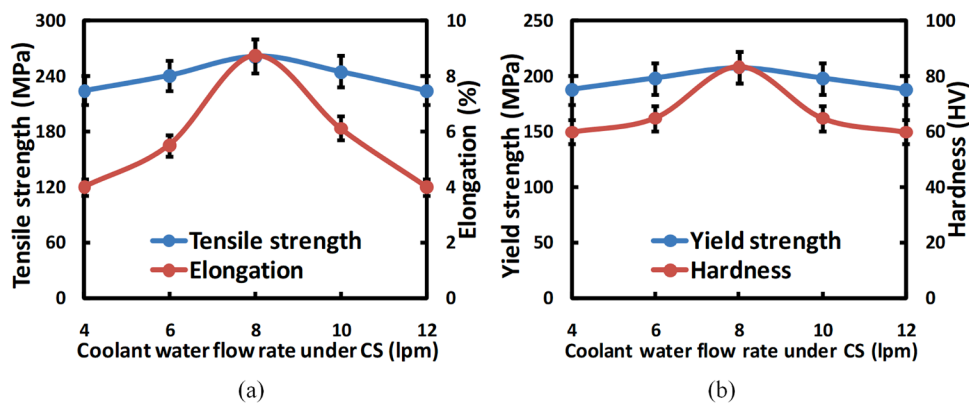

Fig. 4. Mechanical properties of semisolid castings relating coolant water flow rates (underside cooling slope) with (a) tensile strength/elongation and (b) yield strength/hardness

3.2. Impact of coolant water temperature underside cooling slope

For experimental investigation on impact of coolant water temperature underside cooling slope on solidification with microstructure and mechanical properties, conscientious tests got carried out with generation of AZ91 alloy slurry (at slope outlet) for five diverse coolant water temperatures (15, 20, 25, 30 and 35°C) underside cooling slope. Elevated coolant water temperature concerns more slurry temperature at slope outlet. Magnitude of solidification declines with upsurge in coolant water temperature owing to taking away of less heat by coolant water during the process. Therefore, solid fraction decreases with increase in coolant water temperature underside cooling slope. TABLE 2 sums up temperature with solid fraction summary of alloy slurry released from slope outlet at five diverse coolant water temperatures underside cooling slope.

3.2.1. Microstructure of semisolid castings

5 different castings were obtained at five different coolant water temperatures underside cooling slope. Samples were prepared to capture micrographs for metallographic study. Fig. 5 illustrates representative microstructures of mould castings of

TABLE 2

Temperature with solid fraction summary of AZ91 alloy slurry released from slope outlet at five diverse coolant water temperatures underside cooling slope

Coolant water temperature underside cooling slope (°C)	T_{outlet} (°C)	Solid fraction by Scheil equation (%)
15	574	35
20	577	30
25	582	24
30	591	17
35	595	8

AZ91 alloy. It only discloses about variations in pragmatic morphology of castings obtained at different coolant water temperatures underside cooling slope.

3.2.2. Microstructural properties of semisolid castings

Fig. 6 shows structural characterization of previously depicted mould castings microstructures of AZ91 alloy. Pragmatic that initially grain size, shape factor and primary α-phase fraction increase with coolant water temperature till 25°C and then trend reverses. Whilst, grain density reduces with increase in coolant water temperature till 25°C and then trend reverses.
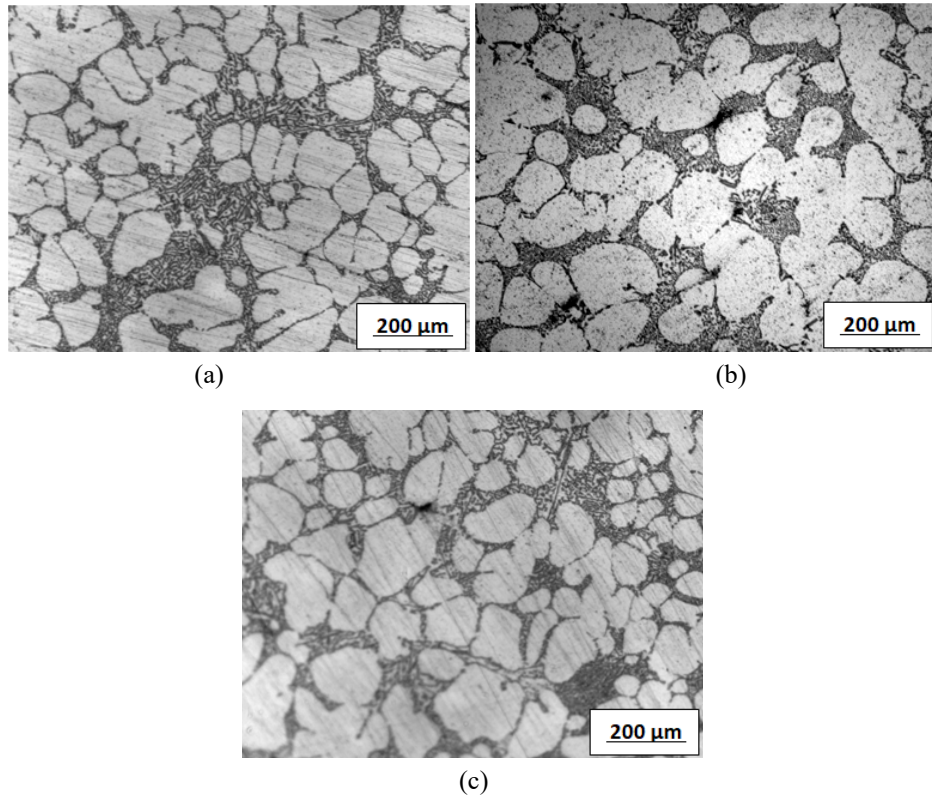
Fig. 5. Microstructures of semisolid castings observed at coolant water temperatures (underside cooling slope) of (a) 15°C, (b) 25°C and (c) 35°C
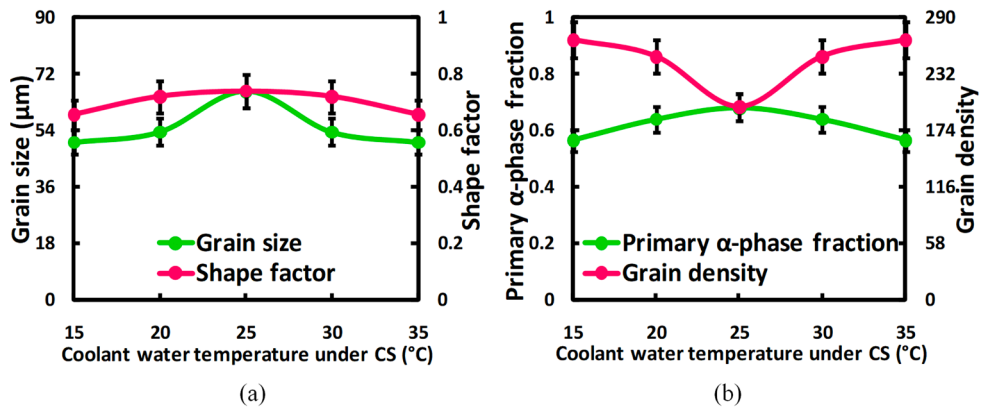

Fig. 6. Microstructural properties of semisolid castings relating coolant water temperatures (underside cooling slope) with (a) grain size/shape factor and (b) α-phase fraction/grain density
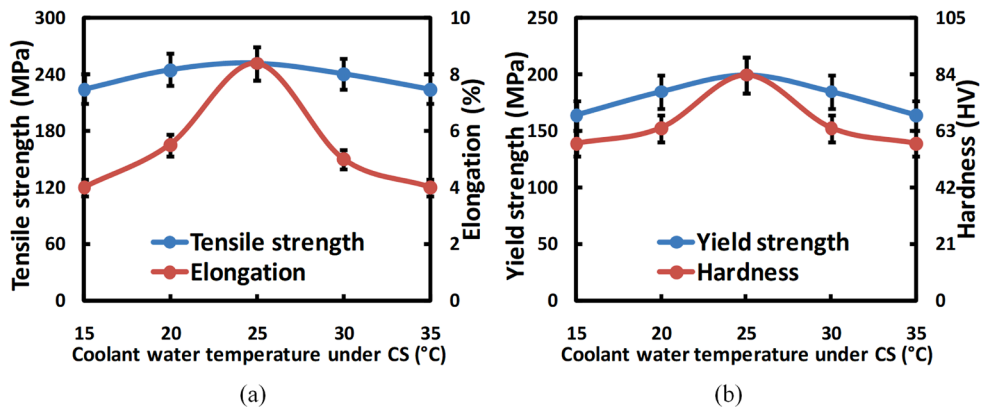

Fig. 7. Mechanical properties of semisolid castings relating coolant water temperatures (underside cooling slope) with (a) tensile strength/elongation and (b) yield strength/hardness

As, firstly, shearing decreases with increase in coolant water temperature underside cooling slope on account of low solidification magnitude. But, afterward, shearing increases with coolant water temperature underside cooling slope on account of high solidification magnitude. Ultimately, favored microstructure got realized at 25°C coolant water temperature with grain size, shape factor, primary α-phase fraction and grain density of 63 μm, 0.71, 0.68 and 198, respectively.

3.2.3. Mechanical properties of semisolid castings

Fig. 7 shows mechanical properties of semisolid castings of AZ91 alloy. Pragmatic that initially strength, elongation and hardness increase with coolant water temperature till 25°C thereafter trend reverses. Mainly it happens due to influence of grain refinement on mechanical properties that gets fully realized from Hall-Petch effect. Certainly, homogeneous grain distribution along with higher primary α-phase fraction (resulting from moderate cooling, solidification together with grain growth and better dissolution of constituent particles) causes higher strength, whilst, higher shape factor and/or homogeneity causes higher ductility. Ultimately, superior mechanical properties got realized at 25°C coolant water temperature with tensile strength, elongation, yield strength and hardness of 250 MPa, 8%, 192 MPa and 80 HV, respectively.

4. Conclusions

Comprehensive experiments conducted for studying impact of coolant water flow rate and coolant water temperature underside cooling slope on solidification and structural characteristics of casted AZ91 Mg alloy. Coolant water flow rate with coolant water temperature underside cooling slope ensure necessary solidification and shear for generating AZ91 semisolid slurry. AZ91 Mg alloy slurry at 5 different coolant water flow rates (4, 6, 8, 10 and 12 lpm) and at five different coolant water temperatures (15, 20, 25, 30 and 35°C) underside cooling slope are delivered inside metal mould. Modest coolant water flow rate of 8 lpm with coolant water temperature of 25°C (underside cooling slope) results fairly modest solidification that would enormously contribute towards improved structural properties. Since, relatively smaller/bigger coolant water flow rate/temperature underside cooling slope would reason some shearing that causes inferior structural properties Eventually, preferred microstructure was obtained at 8 lpm coolant water flow rate and 25°C coolant water temperature underside cooling slope with grain size, shape factor, primary α-phase fraction and grain density of 63 μm, 0.71, 0.68 and 198, respectively. Correspondingly, enhanced mechanical properties were obtained at 8 lpm coolant water flow rate and 25°C coolant water temperature underside cooling slope with tensile strength, elongation, yield strength and hardness of 250 MPa, 8%, 192 MPa and 80 HV, respectively. Hence, modest magnitudes of cooling slope parameters lead to superior structural properties.

REFERENCES

[1] G.W. Form, J.F. Wallace, Typical microstructure of cast metals, Trans. AFS. **68**, 145-156 (1960).

[2] J. Campbell, Solidification technology in the foundry and cast-house, Metals Soc. 61-64 (1981).

[3] G.S. Cole, A.M. Sherman, Light weight materials for automotive applications, Mater. Charact. **35**, 3-9 (1995).

[4] T.M. Yue, G.A. Chadwick, Squeeze casting of light alloys and their composites, J. Mater. Process. Technol. **58**, 302-307 (1996).

[5] E.M. Gutman, Ya. Unigovski, M. Levkovich, Z. Koren, E. Aghion, M. Dangur, Influence of technological parameters of permanent mold casting and die casting on creep and strength of Mg alloy AZ91D, Mater. Sci. Eng. A **234-236**, 880-883 (1997).

[6] N.A.E. Mahallawy, M.A. Taha, E. Pokora, F. Klein, On the influence of process variables on the thermal conditions and properties of high pressure die-cast magnesium alloys, J. Mater. Process. Technol. **73**, 125-138 (1998).

[7] J.C. Gebelin, M. Suery, D. Favier, Characterisation of the rheological behaviour in the semi-solid state of grain-refined AZ91 magnesium alloys, Mater. Sci. Eng. A **272**, 134-144 (1999).

[8] P.J. Blau, M. Walukas, Sliding friction and wear of magnesium alloy AZ91D produced by two different methods, Tribol. Int. **33**, 573-579 (2000).

[9] T. Haga, S. Suzuki, Casting of aluminum alloy ingots for thixoforming using a cooling slope, J. Mater. Process. Technol. **118**, 169-172 (2001).

[10] Z. Fan, Semisolid metal processing, Int. Mater. Rev. **47**, 49-85 (2002).

[11] F. Czerwinski, Assessing capabilities of thixomolding system in semisolid processing of magnesium alloys, Int. J. Cast Met. Res. **16**, 389-396 (2003).

[12] A. Muumbo, H. Nomura, M. Takita, Casting of semi-solid cast iron slurry using combination of cooling slope and pressurisation, Int. J. Cast Met. Res. **17**, 39-46 (2004).

[13] Z. Fan, Development of the rheo-diecasting process for magnesium alloys, Mater. Sci. Eng. A **413-414**, 72-78 (2005).

[14] P. Zhao, H. Geng, Q. Wang, Effect of melting technique on the microstructure and mechanical properties of AZ91 commercial magnesium alloys, Mater. Sci. Eng. A **429**, 320-323 (2006).

[15] Y. Birol, A357 thixoforming feedstock produced by cooling slope casting, J. Mater. Process. Technol. **186**, 94-101 (2007).

[16] E.C. Legoretta, H.V. Atkinson, H. Jones, Cooling slope casting to obtain thixotropic feedstock II: observations with A356 alloy, J. Mater. Sci. **43**, 5456-5469 (2008).

[17] X.R. Yang, W.M. Mao, C. Gao, Semisolid A356 alloy feedstock poured through a serpentine channel, Int. J. Miner. Metall. Mater. **16**, 603-607 (2009).

[18] T. Haga, R. Nakamura, R. Tago, H. Watari, Effects of casting factors of cooling slope on semisolid condition, Trans. Nonferrous Met. Soc. China **20**, 968-972 (2010).

[19] X.R. Yang, W.M. Mao, B.Y. Sun, Preparation of semisolid A356 alloy slurry with larger capacity cast by serpentine channel, Trans. Nonferrous Met. Soc. China **21**, 455-460 (2011).

[20] R.G. Guan, Z.Y. Zhao, F.R. Cao, C. Lian, C.S. Lee, C.M. Liu, Effects of process parameters on microstructure and properties of AZ91 alloy prepared by cooling/stirring and rolling process, Int. J. Cast Met. Res. **25**, 225-231 (2012).

[21] Z.Y. Zhao, R.G. Guan, Q.S. Zhang, C.G. Dai, C.S. Lee, C.M. Liu, Temperature distribution and its influence on microstructure of alloy AZ31 during semisolid rheo-rolling process, Int. J. Cast Met. Res. **26**, 247-254 (2013).

[22] N.K. Kund, P. Dutta, Numerical study of solidification of A356 aluminum alloy flowing on an oblique plate with experimental validation, J. Taiwan Inst. Chem. Engrs. **51**, 159-170 (2015).

[23] N.K. Kund, P. Dutta, Numerical study of influence of oblique plate length and cooling rate on solidification and macrosegregation of A356 aluminum alloy melt with experimental comparison, J. Alloys Compd. **678**, 343-354 (2016).

[24] R.G. Guan, Z.Y. Zhao, Y.D. Li, T.J. Chen, S.X. Xu, P.X. Qi, Microstructure and properties of squeeze cast A356 alloy processed with a vibrating slope, J. Mater. Process. Tech. **229**, 514-519 (2016).

[25] A.M. Negm, S.A. Abdallah, M. Ibrahim, T.S. Mahmoud, Cooling slope casting of cast iron, Mater. Sci. Eng. Technol. **48**, 1103-1112 (2017).

[26] Y. Li, R. Zhou, L. Li, H. Xiao, Y. Jiang, Microstructure and properties of semi-solid ZCuSn10P1 alloy processed with an enclosed cooling slope channel, Metals **8**, 275 (2018).

[27] A. Kolahdooz, S.A. Dehkordi, Effects of important parameters in the production of Al-A356 alloy by semi-solid forming process, J. Mater. Res. Technol. **8**, 189-198 (2019).

[28] S. Acar, K.A. Guler, Producing non-dendritic A356 and A380 feedstocks: evaluation of the effects of cooling slope casting parameters, Mater. Test. **62**, 1147-1152 (2020).

[29] M.M. Shehata, S.E. Hadad, M.E. Moussa, M.E. Shennawy, Optimizing the pouring temperature for semisolid casting of a hypereutectic Al-Si alloy using the cooling slope plate method, Int. J. Metalcast. **15**, 488-499 (2021).